Landscape Classifications for Landscape Metrics-based Assessment of Urban Heat Island: A Comparative Study

X F Zhao [1, 2, 4], **L Deng** [1, 2], **H N Wang** [1, 2], **L Z Hua** [3], **F Chen** [1, 2]

[1] Key Lab of Urban Environment and Health, Institute of Urban Environment, Chinese Academy of Sciences. Xiamen 361021, China
[2] Xiamen Key Lab of Urban Metabolism. Xiamen 361021, China
[3] Institute of Spatial Information Technology, Xiamen University of Technology. Xiamen, China

Abstract. In recent years, some studies have been carried out on the landscape analysis of urban thermal patterns. With the prevalence of thermal landscape, a key problem has come forth, which is how to classify thermal landscape into thermal patches. Current researches used different methods of thermal landscape classification such as standard deviation method (SD) and R method. To find out the differences, a comparative study was carried out in Xiamen using a 20-year winter time-serial Landsat images. After the retrieval of land surface temperature (LST), the thermal landscape was classified using the two methods separately. Then landscape metrics, 6 at class level and 14 at landscape level, were calculated and analyzed using Fragstats 3.3. We found that: (1) at the class level, all the metrics with SD method were evened and did not show an obvious trend along with the process of urbanization, while the R method could. (2) While at the landscape level, 6 of the 14 metrics remains the similar trends, 5 were different at local turn points of the curve, 3 of them differed completely in the shape of curves. (3) When examined with visual interpretation, SD method tended to exaggerate urban heat island effects than the R method.

1. Introduction

Landscape ecology has much to offer for understanding the spatial pattern of land surface temperature (LST) on multiple scales. In recent years, some studies have been carried out on the landscape analysis of urban thermal patterns. It has been proved useful and valuable in assessing urban heat island (UHI) dynamics and their driving forces [1-4]. Thus it is turning more prevalent in the crossing field of landscape ecology and thermal remote sensing, especially in recent China.

Landscape classification is a basic of landscape analysis. With the prevalence of thermal landscape, several key problems have come forth, which stimulate reflections from the basic rules of landscape ecology. One of the most important problems is how to classify thermal landscape into thermal patches [5]. Current researches used different method of thermal landscape classification, including Weng's standard deviation method (SD) [1-3], Zhao's R method [4] etc. But how did the difference between these methods affect the result of our analysis? To find out the differences between the two methods, a comparative study was carried out in Xiamen using a 20-year winter time-serial Landsat images.

[4] xfzhao@iue.ac.cn

2. Data and methods

2.1. Data

A series of Landsat TM/ETM+ images (Table I) were used and subset to the municipality boundary of Xiamen city. All the images were acquired in winter with a five-year interval and under clear and cloudless weather conditions. All these images were rectified to the UTM projection system (Zone N50), and their thermal bands were resampled to 30 m resolution. After preprocessing, the thermal bands were used to analyze thermal dynamics, while other bands were used to acquire LULC and coastline maps through supervised classification, adjusted according to some base maps and manual interpretation of a SPOT 5 image acquired on 25 December 2006. Figure 1 showed one of these time-series images.

Figure 1. TM image subset of Xiamen city on January 8, 2007

Table 1. Images used in this study

Path	Row	Sensor	Date
119	43	Landsat-5 TM	17 January 1987
119	43	Landsat-5 TM	15 January 1992
119	43	Landsat-5 TM	12 January 1997
119	43	Landsat-7 ETM+	02 January 2002
119	43	Landsat-5 TM	08 January 2007

2.2. Retrieval of LST

The digital numbers (DN) of those thermal bands were converted to at-satellite radiance, using equation (1):

$$L_\lambda = Gain_\lambda \cdot DN_\lambda + Bias_\lambda \tag{1}$$

Where L_λ is at-sensor radiance, $Gain_\lambda$ is the slope of radiance/DN conversion function, and $Bias_\lambda$ is the intercept of the radiance/DN conversion function. Gain and bias values are provided in metadata accompanying each TM/+ETM image [10]. Then the at-sensor radiance was converted to effective at-satellite temperature (T_b), which is also called brightness temperature, using equation (2):

$$T_b = \frac{K_2}{\ln(\frac{K_1}{L_\lambda} + 1)} \tag{2}$$

Where K_2 is calibration constant 2, whose value is 1260.56 for TM and 1282.71 for ETM+; K_1 is calibration constant 1, whose value is 607.76 for TM and 666.09 for ETM+; and L_λ is the same as in Equation (1). The unit of T_b is in K.

Since in this study all the images were acquired under good (cloudless and clear) weather conditions, the effects of atmosphere on brightness could be considered to be spatially uniform. On the other hand, this research focuses on the temperature differences between urban and rural areas, not on the absolute values of LST. Thus the atmospheric correction was not carried out, and LST was equaled to brightness temperature retrieved.

2.3. Classification of thermal landscape

After inversion of LST from TM/ETM+ thermal bands, two methods were used to transform the temperature values into thermal patches separately. For the SD method, we used mean and standard deviation values of different dates, shown in Table 2, to divide the LST values into six intervals.

Table 2. Mean and standard deviation values used in the classification of SD method

date	min	μ -2 σ	μ - σ	μ	μ + σ	μ +2 σ	max	σ
2007.01.08	274.85	283.88	285.2	286.52	287.84	289.16	295.74	1.32
2002.01.02	279.45	287.15	288.27	289.39	290.51	291.63	295.83	1.12
1997.01.12	262.02	283.86	285.01	286.16	287.31	288.46	291.77	1.15
1992.01.15	277.43	280.93	281.8	282.67	283.54	284.41	289.96	0.87
1987.01.17	280.94	287.64	288.56	289.48	290.4	291.32	292.66	0.92

For the R method, a relative land surface temperature index R was used to normalize those land surface temperature values of different dates, which could be calculated as

$$R = \frac{T_{u\mathrm{i}} - T_a}{T_a} \tag{3}$$

Where $T_{u\mathrm{i}}$ is the LST of the i^{th} pixel in the extent of thermal landscape, T_a is the average LST of the whole terrestrial part of Xiamen including both rural and urban area. Then thermal patches were segmented out and classified by thresholds shown in Table 3, the corresponding thermal grades were also defined to describe the relative intensity of thermal anomalies.

Table 3. Thresholds used in thermal patches classification of R method

R value	Classes number	UHI grade
Less than or equal to 0	1	No
0.000 - 0.005	2	Weak
0.000 - 0.010	3	Mid
0.010 - 0.015	4	Intensive
0.015 - 0.020	5	Very intensive
More than 0.020	6	Extremely intensive

2.4. Calculation of landscape metrics

After all the thermal images were turned into classified thermal landscape patches, they were transformed into the format of ArcGIS GRID. The GRID files were input into FRAGSTATS 3.3[6] to compute 20 landscape metrics (Table 4), 6 at class level and 14 at landscape level, for all the five date of images.

Table 4. Landscape metrics used in this study

Metrics	Abbreviations	Level
Class Area	CA	class
Percentage of Landscape	PLAND	class
Number of Patches	NP	class and landscape
Patch Density	PD	class and landscape
Largest Patch Index	LPI	class and landscape
Mean Patch Area	AREA_MN	class and landscape
Area-Weighted Shape Index	SHAPE_AM	landscape
Area-Weighted Fractal Index Distribution	FRAC_AM	landscape
Mean Proximity Index	PROX_MN	landscape
Mean Euclidean Nearest Neighbor Distance Distribution	ENN_MN	landscape
Aggregation Index	AI	landscape
Contagion Index	CONTAG	landscape
Interspersion and Juxtaposition Index	IJI	landscape
Patch Cohesion Index	COHESION	landscape
Shannon's Diversity Index	SHDI	landscape
Shannon's Evenness Index	SHEI	landscape

3. Results

We found that at the class level, all the metrics by SD method were evened and did not show an obvious trend with the process of urbanization, while the R method could. Fig.2 used CA as an example to show this difference. While at the landscape level, the results were quite complicated. Six of the 14 metrics showed similar trends between the two methods, five were different at local turn points of the curves, which are LPI, FRAC_AM, PROX_MN, CONTAG, and COHESION. Fig.3 showed the difference of CONTAG index as an instance. Three of them differed completely in the shape of curves, which are IJI, SHDI (Fig.4) and SHEI. The change curves of SHDI and SHEI were also evened as those class-level metrics in SD method. Since the landscape of thermal pattern did change dramatically along with the process of urbanization, it could be seen that SD method was not quite effective in detecting changes of thermal landscape. Meanwhile, R method always showed clear trends of thermal pattern dynamics.

When examined with visual interpretation (Fig.5), SD method tended to exaggerate the visual effect of urban heat island effect than the R method when they used the same 6-class color system. Since all the five classes from level 2 to 6 belonged to urban heat island area in R method, while only three classes 4-6 belonged to urban heat island in SD method according to their classification system. Plenty of pixels were upgraded in their class levels, when shifting from SD method to R method.

4. Conclusion

A comparative study was carried out in Xiamen using a 20-year winter time-serial Landsat images to examine the differences of thermal landscape classification methods. It was found that the method did have big effects on the further analysis of thermal pattern in urban areas, and should be treated carefully when investigate the changes of urban heat island. SD method was not quite effective in detecting changes of thermal landscape. Meanwhile, R method always showed clear trends of thermal pattern dynamics. These outcomes need be tested in other cities in the future to draw universal conclusions.

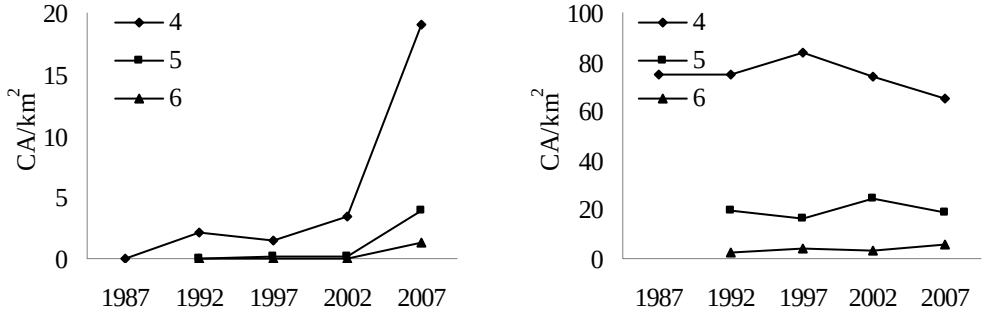

(a) R method (b) Stand Deviation method

Figure 2. Changes of class areas of class 4, 5, 6 at class level in the process of urbanization

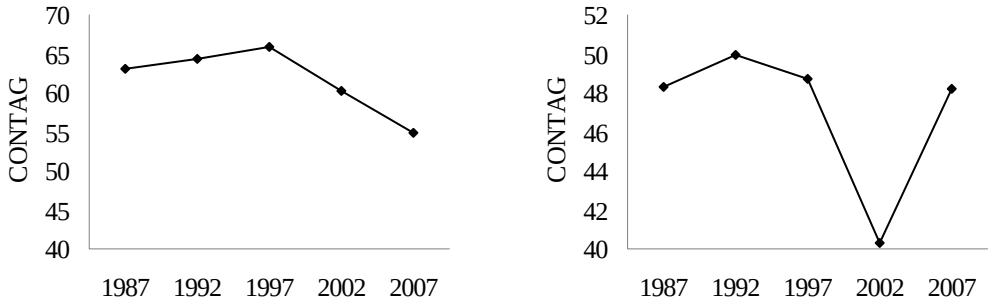

(a) R method (b) Stand Deviation method

Figure 3. Changes of CONTAG index at landscape level in the process of urbanization

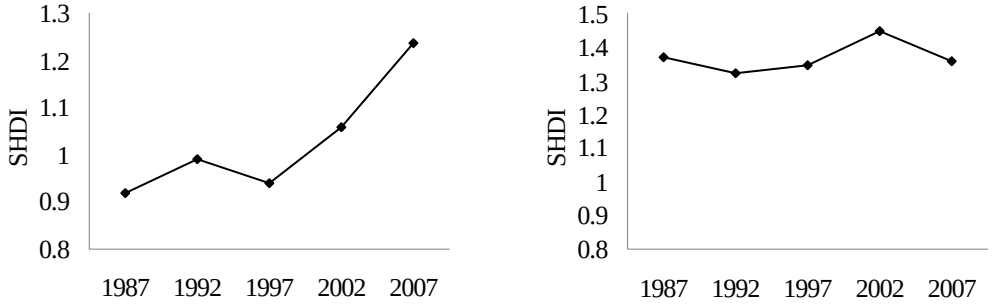

(a) R method (b) Stand Deviation method

Figure 4. Changes of SHDI index at landscape level in the process of urbanization

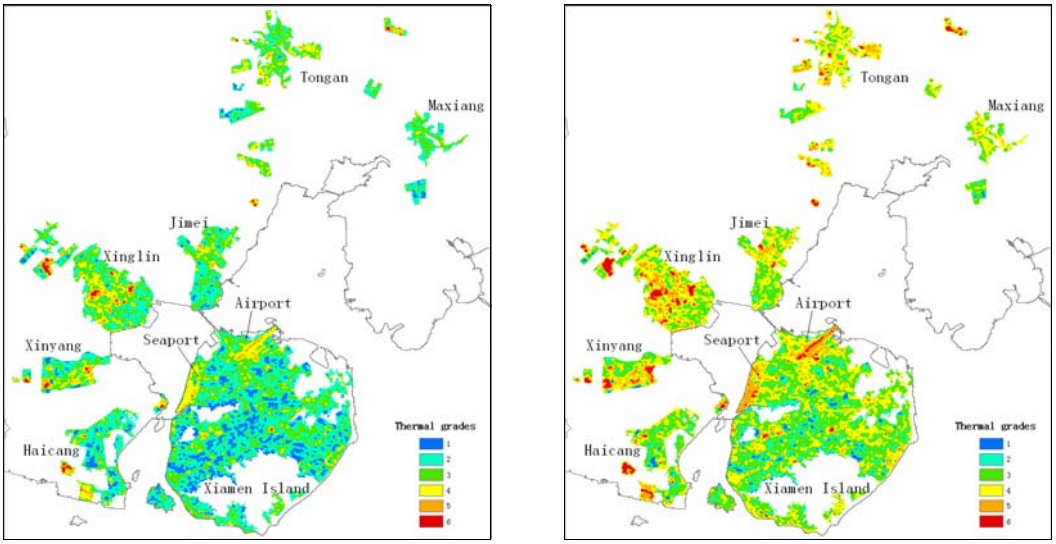

(a) R method (b) Stand Deviation method

Figure 5. Classified thermal landscape on January 8, 2007

References

[1] Weng Q H, Liu H and Lu D S 2007 *Urban Ecosyst.* **10** 203–219
[2] Liu H and Weng Q H 2008 *Environ Monit Assess.* **144** 199–219
[3] Liu H and Weng Q H 2009 *Photogramm. Eng. Rem. S.* **75** 291–304
[4] Zhao X F, Huang J, Ye H, Wang K and Qiu Q Y 2010 *Int. J. Sus. Dev. World* **17** 311-316
[5] Zhao X F, Wang H N, Chen F 2012 *Proc. of 2012 2nd Int. Workshop on Earth Observation and Remote Sensing Applications* (Shanghai: IEEE)
[6] McGarigal K, Cushman S A, Neel M C and Ene E 2002 *Computer software program produced by the authors at the University of Massachusetts, Amherst*, Available from:http://www.umass.edu/landeco/research/fragstats/fragstats.html.

Acknowledgements

This research was supported by the Knowledge Innovation Program of Chinese Academy of Sciences (Y2L0331D50), the National Key Technology R&D Program (No: 2012BAC21B03) and the National Natural Science Foundation of China (No.40901218). We also wish to thank Ms. Jucong Huang and Dr. Lina Tang for their devotions to this research.